Volume 1 | Number 1 | Jan 2013 | Pages 1–100
Soft Matter
www.rsc.org/softmatter
ROYAL SOCIETY OF CHEMISTRY

ARTICLE TYPE www. rsc.org/xxxxxx | XXXXXXXX

Magnetic microrods as tool for microrheology†

Artis Brasovs,[a] Jānis Cīmurs,[a] Kaspars Ērglis,[a] Andris Zeltiņs,[b] Jean-Francois Berret, [c] and Andrejs Cēbers*[a]

Received Xth XXXXXXXXXX 20XX, Accepted Xth XXXXXXXXX 20XX
First published on the web Xth XXXXXXXXXX 200X
DOI: 10.1039/b000000x

Dynamics of superparamagnetic rods in crossed constant and alternating magnetic fields as a function of the field frequency are studied and it is shown that above the critical value of the amplitude of the alternating field the rod oscillates around the direction of the alternating field. The fit of the experimentally measured time dependence of the mean orientation angle of the rod allows one to determine the ratio of magnetic and viscous torques which act on the rod. The protocol of microrheological measurements consists of recording the dynamics of the orientation of the rod when the magnetic field is applied at an angle to the rod and observing its relaxation due to the accumulated elastic energy after the field is switched off. The microrheological data obtained are in reasonable agreement with the macrorheological measurements.

1 Introduction

Application of elongated particles for the study of the viscoelastic properties of the cytoplasm was started in the early fifties by F.H.C.Crick and A.F.W.Hyghes[1,2]. An elongated magnetic particle was oriented by the field starting from the unstressed state and then the field was switched off[1]. The restoration of the orientation angle gave evidence about the elastic properties of the cytoplasm. In the last decade a growth of interest in the application of magnetic rods as a tool for microrheology is observed. Dynamics of the orientation of the elongated magnetic probe in an applied field was studied and viscoelastic properties of the medium measured in[3,4]. Chains of magnetic endosomes were incorporated in the cells and the viscoelastic properties of the cytoplasm were studied by the response of the magnetic probe in an alternating (AC) field applied perpendicularly to the constant field[5]. Later a similar method has been applied for the study of the viscoelastic properties of gels of the bacteriophage Pf1[6]. The macrorheological properties of the Pf1 gels were studied in[7] and a strong effect of the multivalent cations on the viscoelastic properties of the Pf1 gel was found. It should be mentioned that a filamentous virus similar to Pf1 may play an important role in biofilm formation[8]. A review of the properties of filamentous polyelectrolytes similar to the bacteriophage Pf1 is given in[9].

A rotating magnetic field was applied to the study of the viscoelastic properties of complex fluids in[10,11]. The viscoelastic properties of the medium were obtained from the critical frequency of the transition to an asynchronous regime[12,13] and the magnitude of phase slips in this regime. Orientation dynamics of magnetic rods in a constant field were used for the investigation of the properties of viscoelastic fluids in[14–16].

In the present work we develop a new approach to active magnetic microrheology. The characteristics of superparamagnetic rods are determined by studying the orientation dynamics of the rod in an AC field of a sufficiently high frequency applied perpendicularly to the constant field. It is shown that if the amplitude of the AC field is larger than the critical, the mean orientation of the rod is along the AC field. We should mention that this phenomenon is interesting on its own as it enables the manipulation of magnetic microswimmers[17,18] using an AC field.

By fitting the dependence of the orientation angle on the amplitude of the AC field the ratio of the magnetic and viscous torques in the fluid with known viscosity is determined. The obtained parameter of the magnetic rod is used to measure the viscoelastic properties of the gel. It is carried out by using the protocol of F.Crick[1,2] according to which the magnetic field instantaneously changes its direction by the angle $\pi/4$ and is kept constant for a sufficiently small duration of time, when the change of the orientation angle of the rod is small enough. Then the magnetic field is switched off and the relaxation of the rod towards its initial orientation due to the accumulated elastic energy is recorded. This protocol of the measurement is applied to Pf1 gels of different concentrations and to different concentrations of the added $MgCl_2$ salt.

[a] *Faculty of Physics and Mathematics, University of Latvia, Zeļļu-8, Rīga, LV-1021, Latvia*
[b] *Latvian Biomedical Research and Study Center, Ratsupites-1, Rīga, LV-1067, Latvia*
[c] *Matiere et Systemes Complexes, UMR 7057 CNRS Universite Denis Diderot Paris-VII, Batiment Condorcet 10 rue Alice Domon et Leonie Duquet,F-75205 Paris, France*
* *E-mail:aceb@tok.sal.lv*

2 Superparamagnetic rod in constant and perpendicular AC magnetic fields

2.1 Theoretical model

The equation of motion for a superparamagnetic rod in the magnetic field $\vec{H} = (H_\perp \cos(\omega_H t), 0, H_\parallel)$ with the unit vector $\vec{n} = (\sin(\varphi), 0, \cos(\varphi))$ is obtained from the balance of the viscous and magnetic torques acting on the rod which read

$$-\zeta\dot{\varphi} + (\chi_\parallel - \chi_\perp)V(H_\perp \sin(\varphi)\cos(\omega_H t) + H_\parallel \cos(\varphi)) \quad (1)$$
$$(H_\perp \cos(\varphi)\cos(\omega_H t) - H_\parallel \sin(\varphi)) = 0\ ,$$

where for the long rod $\chi_\parallel = \chi$, $\chi_\perp = \chi/(1+2\pi\chi)$ and χ is the magnetic susceptibility of the material of the rod. An illustration of the problem is shown in Fig. 1. Eq.(1) introducing the

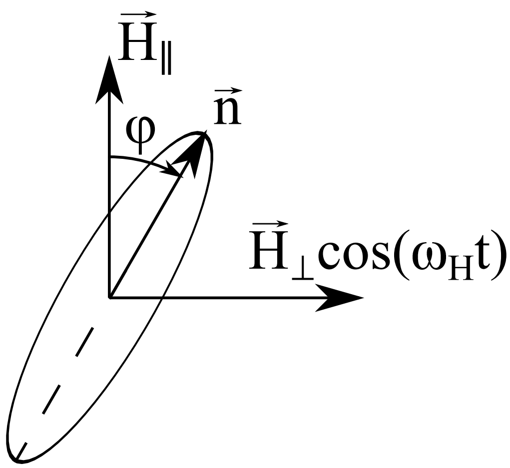

Fig. 1 Magnetic rod in crossed constant and AC magnetic fields.

parameters $h = H_\perp/H_\parallel$, $\omega_c = (\chi_\parallel - \chi_\perp)VH_\parallel^2/\zeta$, dimensionless time $\tilde{t} = \omega_H t$ and $\tilde{\varphi} = 2\varphi$ (tildes are omitted from now on) may be rewritten as follows

$$\dot{\varphi} = -\frac{\omega_c}{\omega_H}\Big(\sin(\varphi)(1 - \frac{1}{2}h^2) \quad (2)$$
$$-\frac{1}{2}h^2\cos(2t)\sin(\varphi) - 2h\cos(t)\cos(\varphi)\Big)\ .$$

Solutions of Eq.(2) may be analysed for two limiting cases: 1) $\omega_c/\omega_H << 1$ and 2) $\omega_c/\omega_H >> 1$. In the first case, which corresponds to the high frequency of an AC field, there are two time scales in the problem - a fast timescale corresponding to the period of the oscillating field and a slow timescale determined by the magnetic torque on the particle $t_s = \omega_c/\omega_H t$. In this case equations are derived for the change of the orientation angle of the rod in the slow time scale where the fast oscillations are averaged out. This gives the mean orientation angle of the rod. The solution of Eq.(2) up to first order terms in a small parameter ω_c/ω_H reads

$$\varphi = \varphi_0(t_s) + \frac{\omega_c}{\omega_H}(A(t_s)\cos(t) + B(t_s)\sin(t) + C(t_s)\sin(2t)) \quad (3)$$

and is satisfied up to first order terms in ω_c/ω_H if

$$\dot{\varphi}_0 = -\sin(\varphi_0)\Big(1 - \frac{1}{2}h^2\Big) \quad (4)$$

and

$$A = 0;\ B = 2h\cos(\varphi_0);\ C = \frac{1}{4}\sin(2\varphi_0)$$

As a result the solution of Eq.(2) reads

$$\varphi = \varphi_0 + \frac{\omega_c}{\omega_H}\Big(2h\cos(\varphi_0)\sin(t) + \frac{1}{4}h^2\sin(2\varphi_0)\sin(2t)\Big) \quad (5)$$

where Eq.(4) describes the evolution of the mean orientation angle of the rod φ_0 in the slow time scale. Two last terms in relation (5) describe the fast oscillations of the rod around its mean orientation. Eq.(4) shows that for $h < \sqrt{2}$ the mean orientation angle tends to $\varphi_0 = 0$ and for $h > \sqrt{2}$ goes to 90^o. It means that for high values of the AC field in the limit of high frequency the rod oscillates around the direction of the AC field.

Solution (5) has been checked by the numerical solution of Eq.(2). In Fig. 2 the solutions of Eq.(2) for particular moments of time are shown by open circles at $\omega_c/\omega_H = 0.01$ and $h = 1.6$ and the numerical solution of Eq.(4) by the solid line. We see that solution (5) agrees very well with the numerical solution.

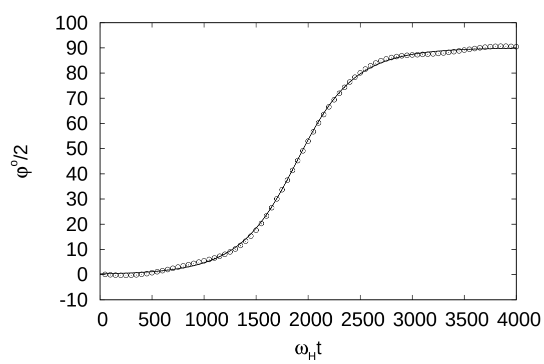

Fig. 2 Dynamics of the rod orientation angle at high frequency of AC field. Open circles - solution of Eq.(2), solid line - solution of Eq.(4). $\omega_c/\omega_H = 0.01$, $h = 1.6$.

In the limit of low frequency of the AC field Eq.(2) put in the form

$$\dot{\varphi} = \frac{\omega_c}{\omega_H}p(t,\varphi)\ , \quad (6)$$

where $p(t,\varphi) = -\sin(\varphi)(1-h^2\cos^2(t)) + 2h\cos(t)\cos(\varphi)$, shows that in the limit of low frequencies the orientation angle jumps between stable solutions of the equation $p(t,\varphi) = 0$ ($\partial p(t,\varphi)/\partial\varphi < 0$). The comparison of the solution of the equation $p(t,\varphi) = 0$ with the numerical solution of Eq.(2) is shown in Fig. 3.

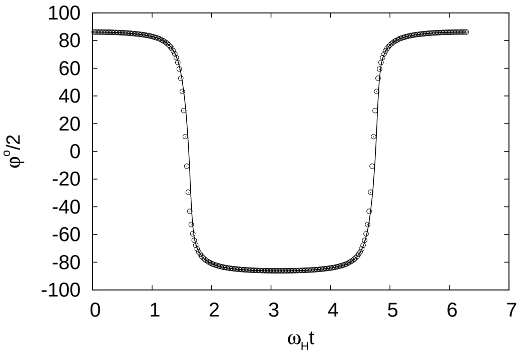

Fig. 3 Dynamics of the rod orientation angle at low frequency of the AC field. Open circles denote solutions of equation $p(t,\varphi) = 0$, the solid line depicts the numerical solution of Eq.(2). $\omega_c/\omega_H = 20$, $h = 15$.

The solution of Eq.(4) reads

$$\ln(|\tan(\varphi_0)|) = \lambda t + C\ , \tag{7}$$

where $\lambda = -\omega_c/\omega_H(1-h^2/2)$, and the constant C is determined by the initial conditions. In the real experiment it is necessary to take into account the presence of the stray magnetic field. The calculation for the time dependence of the mean orientation angle in the magnetic field $\vec{H} = (H_\perp\cos(\omega_H t) + H_0, 0, H_\parallel)$ gives

$$\ln(|\tan(\varphi_0 - \varphi_0^\infty)|) = -\lambda' t + C\ , \tag{8}$$

where

$$\lambda' = \frac{\omega_c}{\omega_H}\sqrt{\left(1+\left(\frac{H_0}{H_\parallel}\right)^2\right)^2 + \frac{1}{4}h^4 - h^2 + \left(\frac{H_0}{H_\parallel}\right)^2 h^2} = \frac{\omega_c}{\omega_H} f(h, H_0/H_\parallel) \tag{9}$$

and

$$\varphi_0^\infty = \frac{1}{2}\arccos\left(\frac{1-h^2/2-H_0^2/H_\parallel^2}{f(h,H_0/H_\parallel)}\right)\ . \tag{10}$$

Dependence of the orientation angle φ_0^∞ on the parameter h is shown in Fig. 4 for several values of the ratio $H_0/H_\parallel$.

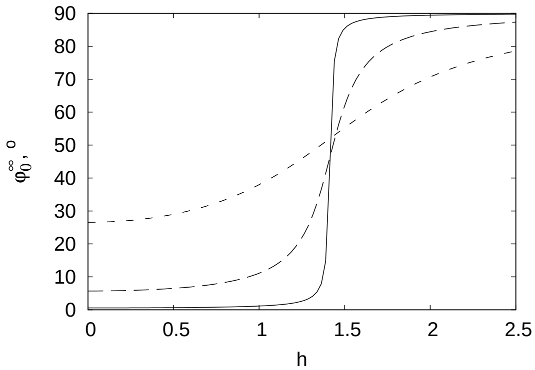

Fig. 4 Stationary orientation angle φ_0^∞ as a function of the dimensionless AC magnetic field strength $h = H_\perp/H_\parallel$ for different values of the stationary field strength H_0. $H_0/H_\parallel = 0.5$ - dashed line, $H_0/H_\parallel = 0.1$ - long dashed line, $H_0/H_\parallel = 0.01$ - solid line.

The rotational drag coefficient of an ellipsoid with a long and short axis a and b respectively is given by $\zeta = \alpha\eta V$, where η is the viscosity of the fluid, V is the volume of the particle and α reads

$$\alpha = 8\pi\frac{a^2+b^2}{a^2N_1+b^2N_2}\ .$$

$N_{1,2}$ are the demagnetization coefficients of the ellipsoid along the long and short axis respectively and are equal to ($e^2 = 1-b^2/a^2$)

$$N_1 = \frac{2\pi(1-e^2)}{e^3}\left(\ln\left(\frac{1+e}{1-e}\right) - 2e\right);\ N_2 = \frac{4\pi - N_1}{2}\ .$$

As a result the critical frequency ω_c is given by the expression

$$\omega_c = \frac{2\pi\chi^2 H_\parallel^2}{(1+2\pi\chi)\alpha\eta}\ . \tag{11}$$

Thus measurement of the ω_c allows one to determine the parameter $F = 2\pi\chi^2/((1+2\pi\chi)\alpha)$. Taking for the magnetic susceptibility of the rod the value $\chi = 0.27$[10] for the ellipsoid with an axis ratio of 18 we obtain the theoretical value of the parameter $F = 8.1\cdot 10^{-4}$.

2.2 Experiment

In the experiments described here all superparamagnetic rods were synthesized according to the method detailed in[19]. Dynamics of the superparamagnetic rod at different values of the parameter h were studied by applying impulses of the AC field (frequency 50 Hz) with increasing amplitude while keeping a

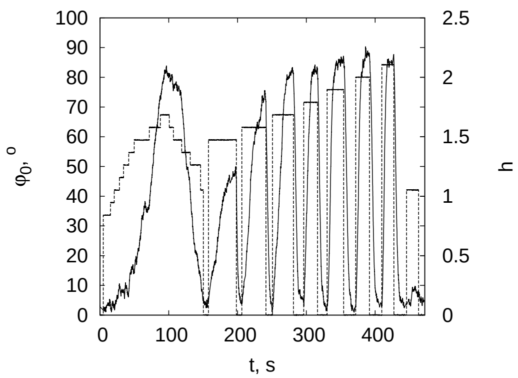

Fig. 5 Experimentally measured mean rotational angle φ_0 of the magnetic particle (solid line and left axis) for different AC magnetic field strengths h (dashed line and right axis) as a function of time.

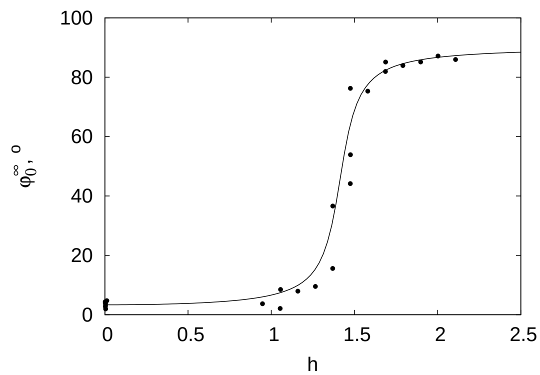

Fig. 7 Orientation angle φ_0^∞ dependence on the parameter $h = H_\perp/H_\parallel$ in experiment. Full circles denote experimental data obtained from a fit to equation (8). The solid line shows a fit to equation (10), using the parameter $H_0/H_\parallel = 0.06$.

constant value of $H_\parallel = 18$ Oe. The orientation angle as a function of time for different values of h is shown in Fig. 5. The angle as a function of time for particular values of the parameter $h = 1.58$ is shown in Fig. 6 and is fitted by the relation (8). The fit gives the parameters φ_0^∞ and λ' and allows us to determine ω_c/ω_H and $H_0/H_\parallel$. The results of the fits are shown in

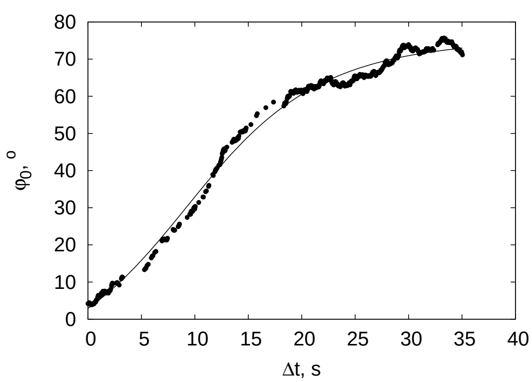

Fig. 6 Mean rotational angle φ_0 of the magnetic particle in the region of a constant ratio $h = 1.58$, where $t \in (206s, 241s)$ as a function of the time interval Δt from the beginning of the interval. Full circles denote the experimental data. The solid line shows the fit of (8) with the parameters $\varphi_0^\infty = 75.3$, $\lambda' = 0.12$ s^{-1} and $C = 1.15$.

Fig. 7, where the dependence of the established mean orientation angle on the parameter h is given. As one can see the experimental data correspond to the predicted critical value of the parameter $h = \sqrt{2}$ very well.

Fitting the experimental results for 10 rods with the close axis ratio approximately equal to 18 for the parameter F gives $F = 4.7 \cdot 10^{-5}$, where for the viscosity the value of the viscosity of water is taken. The value of the parameter F obtained in the experiment is smaller than the theoretical prediction by an order of magnitude. This difference is due to enhanced rotational drag on the rod due to its settling near the bottom of the cell under the action of the gravity force. Since settling does not occur in the gel then for extraction of its properties from the micro-rheological experiments we take the theoretical value of the parameter $F = 8.1 \cdot 10^{-4}$.

From the fitted value of $H_0/H_\parallel = 0.06$ it is found that $H_0 = 1.1$ Oe, which is larger than the horizontal component of the Earth's magnetic field in Rīga $H_{\text{Rīga}} \approx 0.16$ Oe[20] and comes from the stray fields of the equipment.

3 Dynamics of superparamagnetic rod in viscoelastic gel

3.1 Theoretical model

The rods characterized in Section II are used to determine the viscoelastic properties of the gel by studying the relaxation of the rod orientation after releasing the acting torque in the deformed state of the gel. The geometry of the experiment is explained in Fig. 8. After the application of the magnetic torque for the time interval T, which was chosen sufficiently small so that the change of the orientation angle of the rod is small enough, the field ($H_0 = 36$ Oe) is switched off and the relaxation of the orientation angle due to the accumulated elastic energy is registered.

The dynamics of the orientation angle is described by the

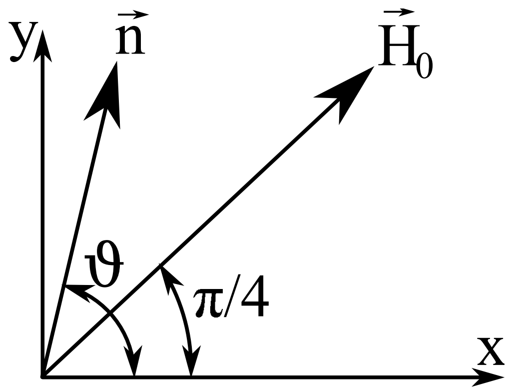

Fig. 8 Sketch of the microrheological experiment. The magnetic rod is initially oriented along the y axis by the application of the magnetic field. At some moment the magnetic field is switched to a new direction making an angle of $\pi/4$ with the y axis. The time duration T of the application of the switched magnetic field is chosen to be small enough to ensure that during this time interval the magnetic torque acting on the particle is practically constant. During this time interval the angle ϑ changes from $\vartheta \simeq \pi/2$ to some value $\vartheta < \pi/2$. After time T the magnetic field is switched off and the relaxation process of the angle ϑ to a value close to the initial is registered.

Jeffreys model, where a damper with the viscosity η_0 is in series with a parallel spring with the elastic modulus k and a damper with the viscosity η. In this case the elastic torque acting on the rod is $kV\alpha(\pi/2-\vartheta_2)$ and the viscous torques acting from the dampers are $-\eta V\alpha\dot{\vartheta}_2$ and $M=-\eta_0 V\alpha\dot{\vartheta}_1$ respectively, where $\vartheta=\vartheta_1+\vartheta_2$. The magnetic torque acting on the rod in the setup shown in Fig. 8 reads

$$M_m = \frac{V\pi\chi^2}{1+2\pi\chi}H_0^2\sin(\pi/2-2\vartheta) \tag{12}$$

and turns the rod in the direction of applied magnetic field. The equation for the orientation angle of the rod is obtained from the balance of torques acting on the rod $M+M_m=0$, which gives the equation

$$\dot{M}\left(1+\frac{\eta}{\eta_0}\right) = -kV\alpha\dot{\vartheta} - \eta V\alpha\ddot{\vartheta} - \frac{k}{\eta_0}M\ . \tag{13}$$

Since the duration of the applied magnetic field was chosen to be fairly short it is possible to consider the case with the constant applied torque determined by the magnetic torque in the initial moment of time when $\vartheta=\pi/2$. The relation (12) gives $M=-V\pi\chi^2H_0^2/(1+2\pi\chi)$ and the dynamics of the rod after switching on the magnetic field are determined by the equation

$$\eta\ddot{\vartheta}+k\dot{\vartheta} = -\frac{k}{\eta_0}\frac{FH_0^2}{2}\ . \tag{14}$$

where F is the parameter introduced in Section II.

The solution of Eq.(14) reads

$$\dot{\vartheta} = -\frac{FH_0^2}{2}\frac{1}{\eta_0}+A\exp(-kt/\eta)\ . \tag{15}$$

The angular velocity of the rod at the initial moment of time $\dot{\vartheta}(0)$ is obtained by integration of Eq.(13) in the time interval $[-\varepsilon;\varepsilon]$ where due to the switching of the direction of the magnetic field $\dot{M}$ is large and taking the limit $\varepsilon\to 0$. This gives

$$\dot{\vartheta}(0) = -\frac{FH_0^2}{2}\left(\frac{1}{\eta}+\frac{1}{\eta_0}\right)\ . \tag{16}$$

As a result we obtain

$$\dot{\vartheta} = -\frac{FH_0^2}{2}\left(\frac{1}{\eta_0}+\frac{1}{\eta}\exp(-kt/\eta)\right) \tag{17}$$

and the angle ϑ is found by the integration. Taking $\vartheta(0)=\pi/2$ we have

$$\vartheta = \frac{\pi}{2}-\frac{FH_0^2}{2}\frac{1}{\eta_0}t-\frac{FH_0^2}{2}\frac{1}{k}\Big(1-\exp(-kt/\eta)\Big)\ . \tag{18}$$

The relation (18) for a small t gives

$$\vartheta = \frac{\pi}{2}-\frac{FH_0^2}{2}\left(\frac{1}{\eta}+\frac{1}{\eta_0}\right)t\ . \tag{19}$$

At the time moment $t=T$ the magnetic field is switched off and the orientation angle of the rod relaxes towards the initial value due to the accumulated elastic energy in the gel. The relaxation process when $M=0$ is described by the equation

$$\ddot{\vartheta}+\frac{k}{\eta}\dot{\vartheta}=0\ , \tag{20}$$

which has the solution

$$\dot{\vartheta} = \dot{\vartheta}(T^+)\exp(-k(t-T)/\eta)\ . \tag{21}$$

The angular velocity of the rod at the initial time moment when the field is switched off is found as previously by the integration of the Eq.(13) in the time interval $[T-\varepsilon;T+\varepsilon]$ where the $\dot{T}$ is large and taking the limit $\varepsilon\to 0$. This gives

$$\dot{\vartheta}(T^+) = \dot{\vartheta}(T^-)+\left(\frac{1}{\eta}+\frac{1}{\eta_0}\right)\frac{FH_0^2}{2}\ . \tag{22}$$

Since according to the solution (17)

$$\dot{\vartheta}(T^-) = -\frac{FH_0^2}{2}\left(\frac{1}{\eta_0}+\frac{1}{\eta}\exp(-kT/\eta)\right) \tag{23}$$

for the angular velocity of the rod we have

$$\dot{\vartheta} = \frac{FH_0^2}{2}\frac{1}{\eta}\Big(1-\exp(-kT/\eta)\Big)\exp(-k(t-T)/\eta)\ . \tag{24}$$

The integration with the initial condition $\vartheta = \vartheta(T^+)$ gives

$$\vartheta = \frac{\pi}{2} - \frac{FH_0^2}{2\eta_0}T - \frac{FH_0^2}{2k}\Big(1-\exp(-kT/\eta)\Big)\exp(-k(t-T)/\eta) \tag{25}$$

The relation (25) may be rewritten as follows

$$\vartheta(t) = \vartheta(T^+) + \frac{FH_0^2}{2k}\Big(1-\exp(-kT/\eta)\Big) \Big(1-\exp(-k(t-T)/\eta)\Big)\,. \tag{26}$$

The relations (19) and (26) are further used in describing the experimental results outlined in the next subsection.

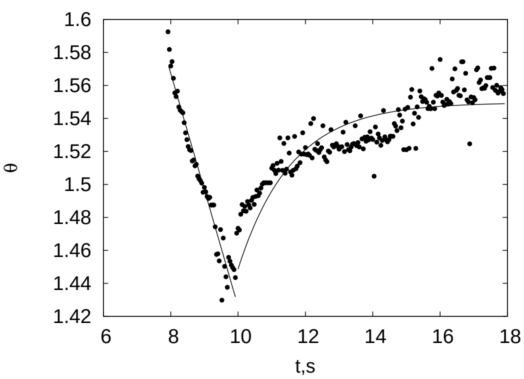

Fig. 9 Time dependence of the orientation angle of the rod when the field is on and off. Concentration of the gel 1 mg/ml.

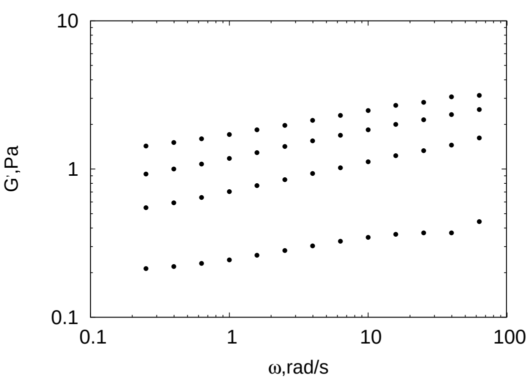

Fig. 10 Storage modulus of the PF1 gel with the concentration 1 mg/ml as a function of frequency for concentrations of the added $MgCl_2$ salt 2; 6; 12; 35 mM. Concentration of salt increases in the upwards direction.

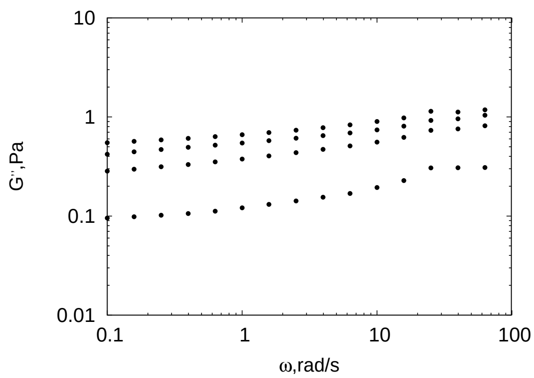

Fig. 11 Loss modulus of the PF1 gel with the concentration 1 mg/ml as a function of frequency for concentrations of the added $MgCl_2$ salt 2; 6; 12; 35 mM. Concentration of salt increases in the upwards direction.

3.2 Experimental results

Experimentally obtained dynamics of the orientation angle of the rod as a function of time is shown in Fig. 9 at $H_0 = 36$ Oe for the particular sample of the PF1 gel with the concentration $c = 1$ mg/ml. Fitting the time dependence when the field is on by the relation (19) as shown in Fig. 9 we obtain $\frac{FH_0^2}{2}\left(\frac{1}{\eta}+\frac{1}{\eta_0}\right) = 0.07$ s^{-1}. By fitting the time dependence of the orientation angle of the rod when the magnetic field is switched off with relation (26) we obtain $k/\eta = 0.63$ s^{-1} and $\frac{FH_0^2}{2k}\Big(1-\exp(-kT/\eta)\Big) = 0.11$. Since $T = 2$ s we have $\frac{FH_0^2}{2\eta} = 0.095$ s^{-1}.

Measurements were carried out for 10 rods with a close axis ratio. The values of the viscosity η and the elastic constant k obtained are $\eta/F = (9.6 \pm 5.2)\cdot 10^2$ $Pa \cdot s$ and $k/F = (5.6 \pm 2.6)\cdot 10^2$ Pa.

In the presence of multivalent cations the storage modulus of the Pf1 gel increases[7]. Our data for the dependence of the storage modulus on the concentration of the $MgCl_2$ salt obtained by the macrorheological measurements with the rheometer are shown in Fig. 10. The loss modulus of the Pf1 gel for the same concentrations of $MgCl_2$ salt is smaller, as shown in Fig. 11, which provides evidence of the gel-like structure of the medium.

It is interesting to check if the results of the macrorheological measurements can be confirmed by the microrheological experiment described above. The dynamics of the rod orientation angle in dependence on time for the Pf1 gel with the concentration $c = 1$ mg/ml at the concentration of the $MgCl_2$ salt 6 mM is shown in Fig. 12. The constants obtained by the fit

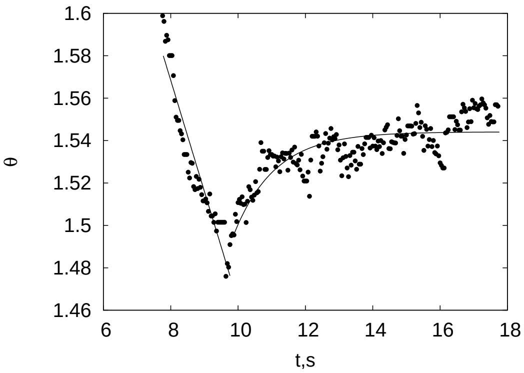

Fig. 12 Time dependence of the orientation angle of the rod when the field is on and off. Concentration of the gel 1 mg/ml, concentration of the $MgCl_2$ salt $c = 6\ mM$.

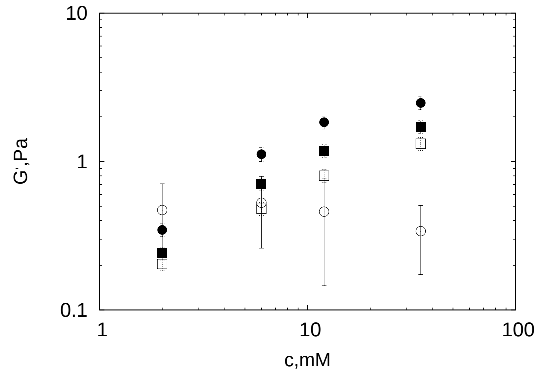

Fig. 13 Comparison of data for the storage modulus for different concentrations of the $MgCl_2$ salt obtained by microrheology (open circles) and macrorheology ($\omega = 10\ rad/s$) (filled circles),($\omega = 1\ rad/s$) (filled squares), ($\omega = 0.1\ rad/s$) (squares). Concentration of the gel 1 mg/ml.

for the particular sample shown in Fig. 12 are $\frac{FH_0^2}{2}\left(\frac{1}{\eta}+\frac{1}{\eta_0}\right) = 0.05\ s^{-1}$; $k/\eta = 0.82\ s^{-1}$ and $\frac{FH_0^2}{2k}\left(1-\exp\left(-kT/\eta\right)\right) = 0.05$. This gives $FH_0^2/2\eta = 0.05\ s^{-1}$ and η_0 significantly greater than η as is usually the case for viscoelastic media[21]. The results of measurements averaged for 10 rods with a close axis ratio for this particular concentration of the $MgCl_2$ salt give $\eta/F = (7.4\pm 2)\cdot 10^2\ Pa\cdot s$ and $k/F = (6.5\pm 3.3)\cdot 10^2\ Pa$.

The microrheological data for the storage modulus may be compared with the macrorheological measurements. Using the value of the parameter F calculated in Section II and the experimentally measured values of k/F on Fig. 13 we plot the elastic modulus k as a function of the salt concentration. On the same Fig. 13 we show the data for the storage modulus obtained by the rheometer for several frequencies of the strain. We see that the agreement between macro- and microrheological measurements at least for the small concentrations of the salt is reasonably good. It is worth noting that the macro- and microrheological data tend to converge with the decrease of the strain frequency of the macro-rheological measurements.

4 Conclusions

It is found that a superparamagnetic rod in crossed constant and AC magnetic fields of sufficiently high frequency at amplitudes of the AC field larger than the critical orientates along the direction of the AC field. Observation of the dynamics in the transitory state gives a novel method for measuring the ratio of the magnetic and viscous torques acting on the microrod. Observation of the orientation angle of the rod in the magnetic field making an angle with the rod and its relaxation due to the accumulated elastic energy after the field is switched off allows one to determine the viscoelastic properties of the Pf1 gel. Values for the storage modulus of the gel obtained from the micro-rheological measurements are in reasonable agreement with the macrorheological measurements for small concentrations of the added salt.

5 Materials and methods

The Pf1 bacteriophage strain (50 mg/ml, 5 w/v percent) was obtained from ASLA Biotech, Riga, containing a 15 mM potassium phosphate buffer at $pH = 7.6$.

5.1 Rheological measurements

For rheological measurements of macroscopic samples the loss moduli and shear storage moduli of 1.2 ml samples with Pf1 at a temperature of 20^oC were measured using the Modular Compact Rheometer MCR 530 (Anton Paar) with the measuring cone CP50-2 (diameter 50 mm, angle 2^o) as a function of frequency using known methods described in detail elsewhere[22]. Specifically, the Pf1 was diluted with a buffer obtaining samples covering the concentration range $0.5\ mg/ml - 5\ mg/ml$.

5.2 Microrheological measurements

For microrheological measurements superparamagnetic rods in the length range of $10-25\ \mu m$ and the diameter range of $0.5-1.5\ \mu m$ were synthesized as described in[19]. The solution of superparamagnetic rods was diluted to a sufficiently low concentration to ensure less than one microrod on average per area of sight in the microscope LEICA DMI 3000 B with an oil immersion objective (100x magnification). The Pf1 was added at a concentration range $0.5\ mg/ml - 5\ mg/ml$, also the $MgCl_2$ salt was used matching the concentrations used in the measurements of macroscopic samples. Samples of $10\ \mu l$ with Pf1 were placed between two microscope coverglass slides separated by a 0.028 mm double stick tape with a $1x1\ cm$ aperture cut out in centre[23]. Measurements using both Pf1 and Pf1 with $MgCl_2$ salt of different concentrations were accomplished using an external AC magnetic field impulse for the orientation of rods at a 45^o angle. The images acquired were processed with MatLab. The viscoelastic properties of gels were obtained from a linear fit (applied impulse) and an exponential fit (relaxation process with no external magnetic field).

5.3 Dynamics in crossed constant and AC magnetic fields

An external AC magnetic field (frequency 50 Hz) was applied using a custom made setup featuring four water-cooled coils with the power supply Kepco BOP 20 10M, managed with a controller NI DAQ card in an impulse mode with increasing amplitude. High resolution images were obtained with a MIKROTRON MC1363 camera at 50 and 25 frames per second. Images were processed with MatLab, obtaining dimensions of rods and the mean orientation angle of the rods as a function of the external field. The Pf1 was diluted with a $MgCl_2$ $1M$ solution to obtain samples with salt concentrations in the range $2\ mM - 75\ mM$. In order to not to over dilute, the concentration threshold value of 10 percent was observed. Each of these samples was used repeatedly increasing the concentration of salt according to the protocol described in[7].

References

1 F.H.C.Crick and A.F.W.Hyghes, *Exp.Cell Res.*, 1950, **1**, 37–80.
2 F.H.C.Crick, *Exp.Cell Res.*, 1950, **1**, 505–533.
3 C.Wilhelm, J.Browaeys, A.Ponton and J.C.Bacri, *Phys.Rev.E*, 2003, **67**, 011504.
4 C.Wilhelm, F.Gazeau and J.C.Bacri, *Phys.Rev.E*, 2003, **67**, 061908.
5 D.Robert, K.Aubertin, J.C.Bacri and C.Wilhelm, *Phys.Rev.E*, 2012, **85**, 011905.
6 K.Erglis, V.Ose, A.Zeltins and A.Cebers, *Magnetohydrodynamics*, 2010, **46**, 23–29.
7 E.M.Huisman, Q. Wen, Y.-H. Wang, K.Cruz, G.Kitenbergs, K.Erglis, A.Zeltins, A.Cebers and P.A.Janmey, *Soft Matter*, 2011, **7**, 7257–7261.
8 J.S.Webb, M.Law and S.Kjelleberg, *J.Bacteriol.*, 2004, **186**, 8066–8073.
9 P.A.Janmey, D.R.Slochower, Y.-H. Wang, Q. Wen and A.Cebers, *Soft Matter*, 2014, **10**, 1439–1449.
10 L.Chevry, N.K.Sampathkumar, A.Cebers and J.-F.Berret, *Phys.Rev.E*, 2013, **88**, 062306.
11 L.Chevry, A.Colin, B.Abou and J.F.Berret, *Biomaterials*, 2013, **34**, 6299–6305.
12 B.Frka-Petesic, K.Erglis, J.-F.Berret, A.Cebers, V.Dupuis, J.Fresnais, O.Sandre and R.Perzynski, *JMMM*, 2011, **323**, 1309–1313.
13 A.Tokarev, B.Kaufman, Y. Gu, T.Andrukh, P.H.Adler and K.G.Kornev, *Applied Physics Letters*, 2013, **102**, 033701.
14 D.B.Allan, D.M.Firester, V.P.Allard, D.H.Reich, K.J.Stebe and R.L.Leheny, *Soft Matter*, 2014, **10**, 7051–7060.
15 P.Dhar, Y.Cao, Th.M.Fischer and J.A.Zasadzinskii, *Physical Review Letters*, 2010, **104**, 016001.
16 M.H.Lee, D.H.Reich, K.J.Stebe and R.L.Leheny, *Langmuir*, 2010, **26**, 2650–2658.
17 R.Dreyfus, J.Baudry, M.L.Roper, M.Fermigier, H.A.Stone and J.Bibette, *Nature*, 2005, **437**, 862–865.
18 A.Cebers, *Magnetohydrodynamics*, 2005, **41**, 63–72.
19 J.Fresnais, J.-F.Berret, B.Frka-Petesic, O.Sandre and R.Perzynski, *Adv.Mat*, 2008, **2008**, 3877–3881.
20 S. Maus, S. Macmillan, S. McLean, B. Hamilton, A. Thomson, M. Nair and C. Rollins, *The US/UK World Magnetic Model for 2010-2015*, National geophysical data center technical report, 2010.
21 Yu.L.Raikher and V.V.Rusakov, *JETP*, 2010, **138**, 998–1005.
22 P.A.Janmey, M.E.McCormick, S.Remmense, J.L.Leight, P.G.Georges and F.C.MacKintosh, *Nature Materials*, 2007, **6**, 48–51.
23 K.Erglis, D.Zhulenkovs, A.Sharipo and A.Cebers, *J.Phys.:Cond.Matter*, 2008, **20**, 204107.